Structure Characterization of Fe-B Amorphous Alloys by a Laboratory EXAFS Spectrometer

Structure Characterization of Fe-B Amorphous Alloys by a Laboratory EXAFS Spectrometer*

Fumitake ITOH, Tomohisa KITANO** and Kenji SUZUKI
The Research Institute for Iron, Steel and Other Metals

(Received January 13, 1986)

Synopsis

The local atomic arrangement for Fe-B amorphous alloys in both as-prepared and mechanically deformed states was investigated by a laboratory EXAFS spectrometer. It was found that the nearest neighbour distance changed drastically at 16 to 18 at% of B atom concentration and that the mechanical deformation(cold rolling and tension) yielded the non-uniform displacement of Fe atoms in Fe-B amorphous alloys, keeping the Fe-B correlation unchanged.

I. Introduction

Much progress has been made to measure the local structure by means of Extended X-ray Absorption Fine Structure(EXAFS) technique[1]. As well known, EXAFS technique gives us the information about the local atomic structure around the specified chemical species of constituent atoms in an amorphous alloy. This feature is in contrast to that of conventional structure analysis techniques such as X-ray, neutron and electron diffraction, in which the structure can be observed in terms of the total radial distribution g(r). In an amorphous binary alloy, the g(r) is a weighted sum over three kinds of partial distribution functions and therefore it is sometimes difficult to separate rigorously the g(r) into three parts. In this respect, EXAFS technique is a unique technique and important to study the local atomic structure in multi-component amorphous alloys.

However, the majority of work in EXAFS have been carried out using the synchrotron radiation source. In fact, the synchrotron radiation source has 10^3-10^4 greater intensity than the conventional X-ray tube. Therefore, the time required to make the EXAFS measurement is reduced from a day to a few minites when the synchrotron radi-

---

* The 1792th report of the Research Institute for Iron, Steel and Other Metals.

**Fundamental Research Laboratories, NEC Corporation, Kawasaki 213.

ation source is used. But, access to the synchrotron radiation source is rather limited to most workers and even so the time allotted is usually quite inadequate.

Meanwhile it has been found that the utilization of the traditional X-ray generator can give us precise EXAFS data with good quality under careful contrivances[2-4]. Therefore, it is still useful to construct a laboratory EXAFS facilities.

In this paper, the EXAFS spectra for $Fe_{100-x}B_x$(x= 14,16,18,20 and 25) amorphous alloys were measured by making use of the laboratory EXAFS spectrometer in order to study the local atomic structure in these alloys. Section II is devoted to the description of present EXAFS spectrometer. The experimental results for Fe-B amorphous alloys will be given in section III and the deformation effects by cold rolling and tension on the EXAFS spectra will be focused in section IV. The conclusions are summarized in section V.

II. Experimental

The EXAFS spectrometer used in this study is shown schematically in Fig. 1. The white beam emitted from a 12 kW rotating Mo anode is monochromatized and focused by a Johannson type monochrometer of Ge (220) plane bent with a radius of the Rowland circle, R= 245 mm.

The X-ray with the wavelength $\lambda = 2d_{220}\sin\theta$(d_{220} is the lattice spacing of the monochrometer, θ is the grazing angle) selected by the monochrometer was then detected by an usual scintillation counter after passing through the sample in θ- 2θ step scan mode. The distance between the divergence slit(D.S.) and the monochrometer and between the monochrometer and the receiving slit(R.S.), l_a and l_s respectively, were chosen to satisfy $\delta l_a = \delta l_s$ to give the minimum angle divergence and $\delta l_a < 0.1\ l_a$ to result in the minimum intensity loss, where $\delta l_a = l_a - 2R\sin\theta$ and $\delta l_s = l_s - 2R\sin\theta$[3]. Both l_a and l_s can be varied from 195 to 475 mm, so that this spectrometer enables us to measure the K_α -EXAFS spectrum from Ti to Ni in the periodic table. The replacement of the monochrometer by LiF(220) (d_{220}= 1.424 A, R= 490 mm) can cover the range of element from Ni to Se. The energy resolution was about 10 eV in full width at half maximum.

The transmitted intensities from the sample(d in thickness) and the monitor(d'in thickness), I_s and I_m respectively, are related to the absorption coefficients of the sample and the monitor, $\mu(E)$ and $\mu'(E)$ respectively, by the following equation,

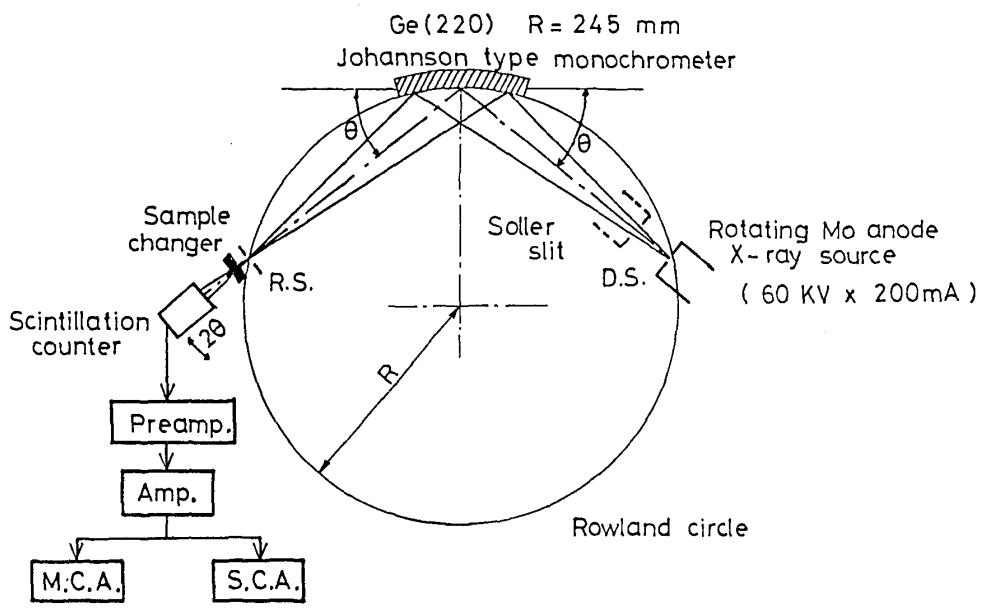

Fig.1 Schematic diagram of EXAFS spectrometer using conventional X-ray source, Johannson type bent crystal monochrometer and scintillation counter.

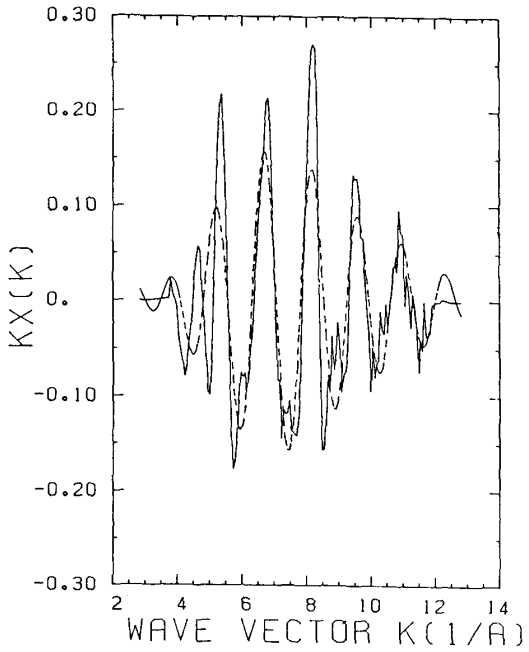

Fig.2 Normalized $k\chi(k)$ for crystalline bcc Fe at room temperature. The dashed curve shows the result of Fourier filtering from the first peak of F(r) in eq.(5).

$$\ln(I_s/I_m) = \mu(E)d - \mu'(E)d' = \chi(E) \frac{\mu_0(E)d}{\mu_0(E)d - \mu_0'(E)d'} \quad (1)$$

The $\chi(E)$ is the so-called EXAFS function defined by

$$\chi(E) = \frac{\mu(E) - \mu_0(E)}{\mu_0(E)} \quad (2)$$

where $\mu_0(E)$ is the absorption coefficient for an isolated atom.

The momentum of photon energy, k, was determined from the energy separation between the absorption edge E_0 and the incident X-ray energy E,

$$k = \sqrt{\frac{2m(E - E_0)}{h^2}} \quad . \quad (3)$$

An example of $k\chi(k)$ obtained for crystalline bcc Fe is shown in Fig.2, which is in agreement with the previous work by Motta et al[5].

The theory for EXAFS phenomena yields the following expression for $\chi(k)$,

$$\chi(k) = \sum \frac{N_j}{kr_j^2} |f_j(k)| \exp(- \frac{2r_j}{\lambda}) \exp(- 2k^2\sigma_j^2) \times \sin(2kr_j^2 + \alpha_j(k)) . \quad (4)$$

Eq.(4) is based upon an assumption that the number of atom N_j is distributed in the gaussian form, the mean square width of which is σ_j^2, in the j-th shell of average radius r_j around the absorbing atom. $|f_j(k)|$ is the backscattering amplitude, $\alpha_j(k)$ is the phase shift experienced by the photoelectron and λ is the mean free path of the photoelectron due to inelastic scattering process.

The structural informations about r_j was extracted from the radial distribution function F(r) obtained as the Fourier transform of $k\chi(k)$,

$$F(r) = \frac{1}{\sqrt{2\pi}} \int_{k_{min}}^{k_{max}} k\chi(k) \exp(2ikr) W(k) dk \quad (5)$$

where W(k) is a window function defined by

$$W(k) = \frac{1}{2} \left[1 - \cos\{2\pi(\frac{k - k_{min}}{k_{max}-k_{min}})\} \right] \quad (6)$$

to prevent the termination effects from the Fourier transformation. Here, k_{min} and k_{max} are minimum and maximum k-values available in this experiments. In this study, k_{min}= 2.8 A^{-1} and k_{max}= 12.8 A^{-1} were used.

III. EXAFS for Fe-B Amorphous Alloys

$Fe_{100-x}B_x$ amorphous samples(x= 14,16,18,20 and 25) were prepared by a rapidly melt-quenching technique using a rotating Cu roll in Ar -gas atmosphere into the shape of continuous ribbon wire with 1 mm in width, 30 μm in thickness and several meters in length. For each EXAFS measurement, the sample thickness was reduced to about 10 μm, corresponding to $\mu(E)d \simeq 1.5$ in the X-ray energy region of interest, to attain the maximum signal to noise ratio[3].

The F(r)'s by eqs.(1)-(6) for Fe-B amorphous alloys are shown in Fig. 3. For comparison, the F(r) for crystalline $Fe_{75}B_{25}$ is shown in Fig. 4. The crystalline sample was obtained by annealing the amorphous $Fe_{75}B_{25}$ at 450°C for 2 hours under vacuum of 10^{-5} Torr.

It can be seen that the radial distribution function F(r) for crystalline $Fe_{75}B_{25}$ is very similar to that for amorphous $Fe_{75}B_{25}$. Although the crystalline $Fe_{75}B_{25}$ thus prepared has been known not to be a single phase of the metastable Fe_3B but a mixture of α-Fe and various compounds, it is interesting to see the similarity of local atomic structure between the crystalline and amorphous $Fe_{75}B_{25}$.

The concentration dependence of the first peak position in the imaginary part of the radial distribution Im(F(r)) is shown in Fig.5. This is because the peak position in Im(F(r)) was found to be less dependent on the termination effect than that in the absolute value F(r).

The first point to be noticed is that the nearest neighbour distance from Fe atom lies around r= 2.02 - 2.05 A in agreement with the previous papers[6-8]. This distance differs considerably from the values r= 2.5 - 2.6 A obtained from X-ray and neutron scattering experiments for Fe-B amorphous alloys[9-10] and also the value r = 2.25 A obtained from the F(r) for crystalline Fe in this study. Although the former fact is not surprizing because the phase factor $\alpha_j(k)$ is not taken into account, it is interesting to note the smaller peak position compared with the crystalline Fe. Haensel et al[6] and Crescenzi et al[7] attributed the first peak in F(r) to Fe-Fe contribution, taking into special account of asymmetry of the nearest neighbour radial distribution originated from the anharmonic effect in amorphous alloys. On the other hand, Cargill showed that EXAFS spectra for $Co_{76}P_{24}$ and $Fe_{80}B_{20}$ amorphous alloys are dominated by metal-metalloid nearest neighbour contributions rather than metal-metal contributions.

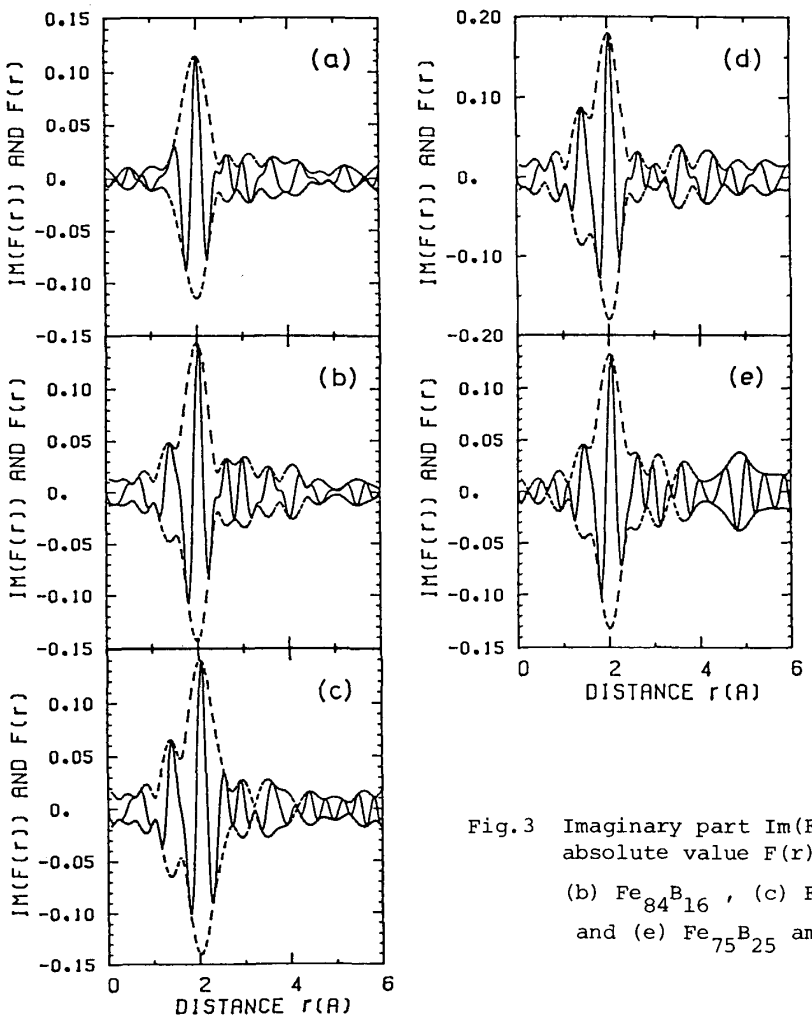

Fig.3 Imaginary part Im(F(r)) (solid line) and absolute value F(r) for (a) $Fe_{86}B_{14}$, (b) $Fe_{84}B_{16}$, (c) $Fe_{82}B_{18}$, (d) $Fe_{80}B_{20}$ and (e) $Fe_{75}B_{25}$ amorphous alloys.

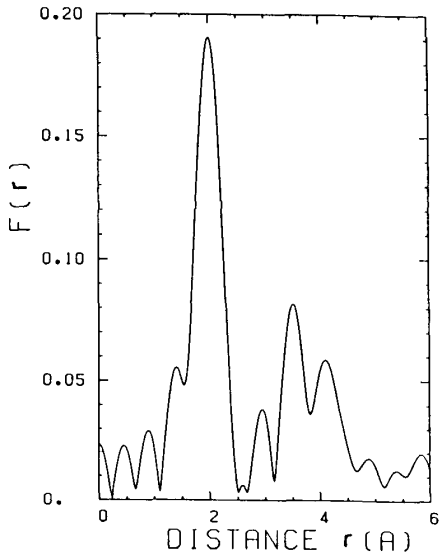

Fig.4 Absolute value F(r) for crystallized $Fe_{75}B_{25}$ alloy.

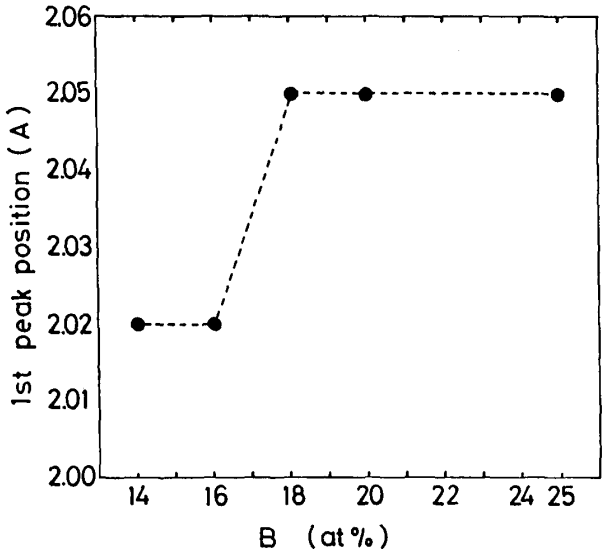

Fig.5 Concentration dependence of the first peak position in Im(F(r)) for Fe-B amorphous alloys.

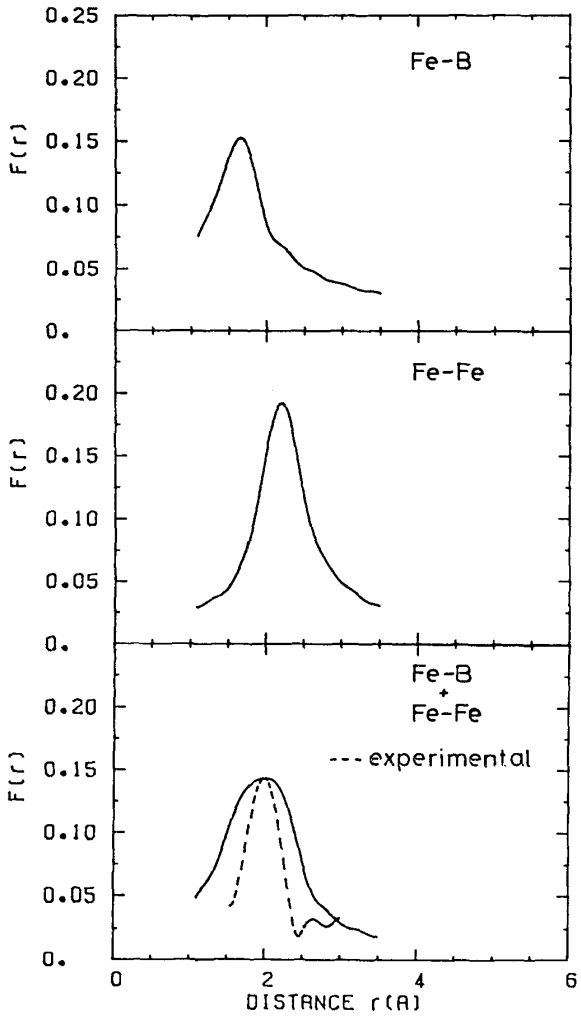

Fig.6 A calculated F(r) for $Fe_{80}B_{20}$ amorphous alloy.

In order to make the situation clearer, a theoretical $\chi(k)$ for amorphous $Fe_{80}B_{20}$ was calculated based upon eq.(4), using the partial structure factors of this alloy obtained by Lamparter et al[10] and the same parameters with those for $Co_{76}B_{24}$ amorphous alloy adopted by Cargill[8]. The theoretical F(r) of this $k\chi(k)$ function are shown in Fig.6 for (a) Fe-B pair, (b) Fe-Fe pair and (c) a weighted sum of Fe-B and Fe-Fe pairs which corresponds to $Fe_{80}B_{20}$ amorphous alloy. Regadless of crude approximation for the EXAFS parameters, a nice agreement of the first peak position between the calculated and the experimental F(r) can be seen. This suggests that the first peak in F(r) can be assigned to an average of Fe-Fe and Fe-B pair correlation in the amorphous alloy.

Another point to be noticed in Fig.5 is that the first peak position changes drastically between 16 and 18 at % of boron content in contrast to the continuous concentration dependence of the Fe-Fe nearest neighbour distance observed by Fukunaga et al[9]. The smaller distance at lower boron concentration can be ascribed to the shorter distance due to the strong chemical bonding between Fe and B atoms. This explanation is consistent with the experimental results of XPS[11] and Mössbauer[12].

IV. Deformation Effect on EXAFS Spectra

One of the most remarkable features of amorphous alloys would be mechanical properties, i.e., high fracture strength, toughness and ductility[13]. Therefore, it is interesting to study the atomic-scale process of mechanical deformation of amorphous alloy by EXAFS measurement.

Cold Rolling

Fe-B amorphous alloys described in the previous section were reduced in thickness by cold rolling along the direction of the long ribbon. The degree of deformation was defined as the relative increase of length.

Figure 7 shows the F(r) for $Fe_{86}B_{16}$ amorphous alloy for various deformation. It can be seen that (a) the first peak position in F(r) is displaced towards higher r-space with increasing the degree of deformation, and (b) the shape of the first peak becomes less asymmetric , being accompanied by the increase of height. The peak position r_p in the F(r) are given in Table I.

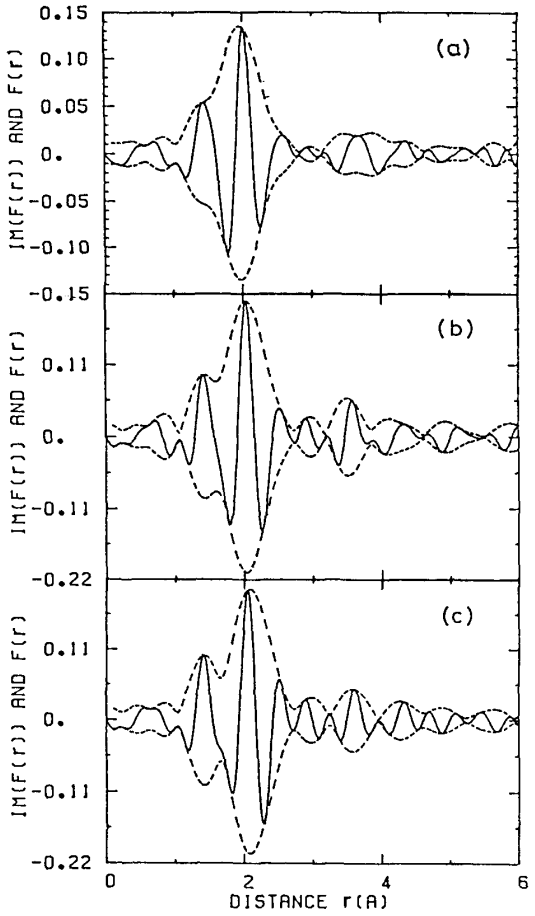

Fig.7 Effect of cold rolling on F(r) for $Fe_{86}B_{14}$ amorphous alloy.

(a) 24 % deduction
(b) 44 % deduction
(c) 59 % deduction

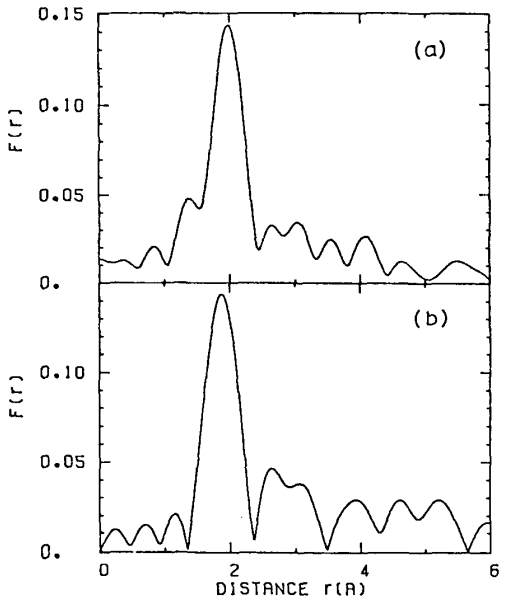

Fig.8 Effect of tension on F(r) for $Fe_{84}B_{16}$ amorphous alloy.

(a) as-prepared
(b) in tension

Table I. Peak Position r_p in Im(F(r)) and absolute F(r) in $Fe_{86}B_{14}$ amorphous alloy by cold rolling.

Degree of deformation (%)		0	24	44	59
r_p in Im(F(r))	(A)	2.02	2.02	2.03	2.06
r_p in F(r)	(A)	2.00	1.97	2.04	2.09

There are two possibilities to explain the shift of the first peak in F(r) towards higher r-space by cold rolling. One is the increase of Fe-Fe interatomic distance due to the introduction of more excess free volume and another is the increase of coordination number of the nearest neighbouring Fe-Fe correlation due to the local densification by the cold rolling. However, according to the neutron diffraction experiment for cold-rolled $Pd_{83}Si_{17}$ amorphous alloy by Hayashi et al[14], it has been found that there is just a little change in the total radial distribution function g(r) without noticeable increase of the coordination number by 52 % cold rolling. Therefore, it would be reasonable to propose the former possibility as the atomic scale mechanism of cold rolling at the present stage.

Tension

An EXAFS spectrum of $Fe_{86}B_{14}$ was measured under a certain tension within the elastic limit. The F(r) is shown in Fig. 8. It is clear that the first peak position in F(r) shifts to the lower r-space by applying the tension in contrast to the previous cold rolling. This fact can be explained by the model proposed above; the Fe atoms surrounding the Fe atom rearrange in a way to reduce the Fe-Fe interatomic distance in compensation for perhaps decrease of free volume.

V. Conclusions

1) Laboratory EXAFS facilities, which consist of conventional rotating anode, Johannson-type monochrometer and scintillation counter, were constructed. Using this facilities, EXAFS spectra for Fe-B amorphous alloys were successfully measured.

2) The concentration dependence of the first peak position in F(r) of Fe-B amorphous alloys is not linear with boron content. This behaviour can be explained by the strong chemical bond formed between Fe and B

atoms, based on the point of view that the first peak in F(r) comes from both metal-metal and metal-metalloid contributions.

3) The cold rolling of $Fe_{86}B_{14}$ amorphous alloy showed the shift of the first peak position towards higher r-space, while the tension of $Fe_{84}B_{16}$ amorphous alloy showed the reverse tendency. These are an indication that the deformation yields non-uniform displacement in the amorphous alloy. A model for atomic-scale process of the cold rolling and tension in Fe-B amorphous alloys was proposed; the Fe-Fe nearest neighbour distance can change in compensation for the excess free volume by the deformation, while the Fe-B nearest neighbour distance remains unchanged.

Acknowledgements

The authors would like to express their thanks to Dr.T.Fukunaga for his kind helps during this study and Dr.T.Kamiyama for his advice in constructing the present EXAFS spectrometer.

This work is supported by the Grant-in-Aid for Scientific Research (Project No.00442036) from the Ministry of Education, Science and Culture.

References

(1)" EXAFS and Near Edge Structure", ed.A.Bianconi, L.Incoccia and S.Stipchich, Springer Verlag, 1983.

(2)" Laboratory EXAFS Facilities-1980", AIP Conference Proceedings No. 64, ed. E.A.Stern, American Institute of Physics, 1980.

(3)G.S.Knapp, H.Chen and T.E.Klippert, Rev.Sci.Instrum. 49(1978), 1658.

(4)K.Tohji and Y.Udagawa, Rev.Sci.Instrum., 54(1983), 1482.

(5)N.Motta, M.De Crescenzi and A.Balzarotti, p103 in ref.(1).

(6)R.Haensel, P.Rabe, G.Tolkiehn and A.Werner, "Liquid and Amorphous Metals", ed. E.Lusher and H.Coufal, Sijthoff & Nordhoff, Alphen aan den Rijn, The Netherland, 1980, p459.

(7)M.De Crescenzi, A.Balzarotti, F.Comin, L.Incoccia, S.Mobilio and N. Motta, Solid State Comm., 37(1981), 921.

(8)G.S.Cargill III, Proceedings of 4th Int.Conf.on Rapidly Quenched Metals, ed.T.Masumoto and K.Suzuki, The Japan Institute of Metals, 1982, p389.

(9)T.Fukunaga, M.Misawa, K.Fukamichi, T.Masumoto and K.Suzuki, Rapidly Quenched Metals III, Vol.2, ed. B.Canter, The Metal Society, London , 1978, p325.

(10)P.Lamparter, E.Nold, G.Rainer-Harback, E.Grallath and S.Steeb, Z.Natureforsh., 36a, (1981), 165.
(11)M.Matsuura, T.Nomoto, F.Itoh and K.Suzuki, Solid State Comm., 33, (1980), 895.
(12)R.Oshima and F.E.Fujita, Jap. Jour. Appl. Phys., 20, (1981), 1.
(13)H.S.Chen, Rep. Prog. Phys. 43, (1980), 353.
(14)N.Hayashi, T.Fukunaga, N.watanabe and K.Suzuki, KENS Report III, ed. Y.Ishikawa, N.Niimura and S.Ikeda, 1982, National Laboratory for High Energy Physics(Japan), p 17.